Swanson et al., http://www.jcb.org/cgi/content/full/jcb.201306073/DC1

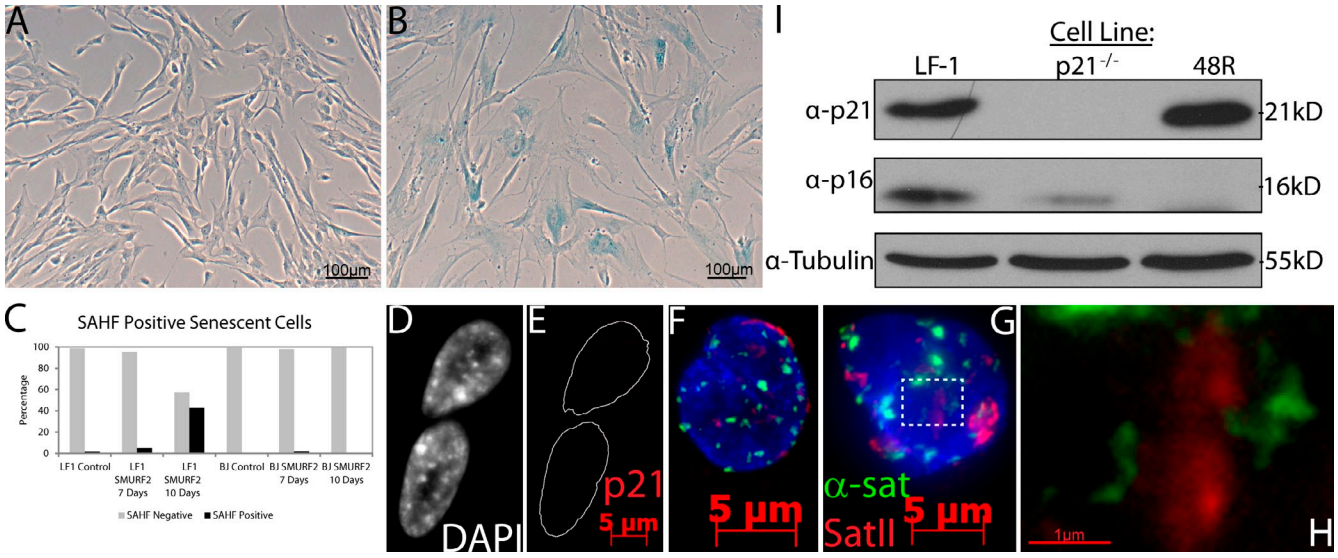

Figure S1. **SADS is a property common to many different senescence models and pathways.** (A and B) β-Gal staining shows that LF1 fibroblasts infected with SMURF2 (B) are senescent, whereas cells infected with a control (A) are not. (C) Percentage of BJ and LF1 cells with SAHF plotted as an independent variable (n = 200, representative of one of three repeats). (D and E) p21 staining (red) is not present in LF1 p21 knockout senescent cells as judged by the presence of SAHF (DAPI; negative antibody control). (F–H) SADS form in human breast epithelial p16 knockout cells as judged by distended α-sat (green) and sat II (red; G) and blown up in H, while others have tight satellite signals indicative of cycling cells (F). (I) Western blot demonstrating that senescent LF1 $p21^{-/-}$ and 48R mammary epithelial cells lack p21 and p16 expression, respectively.

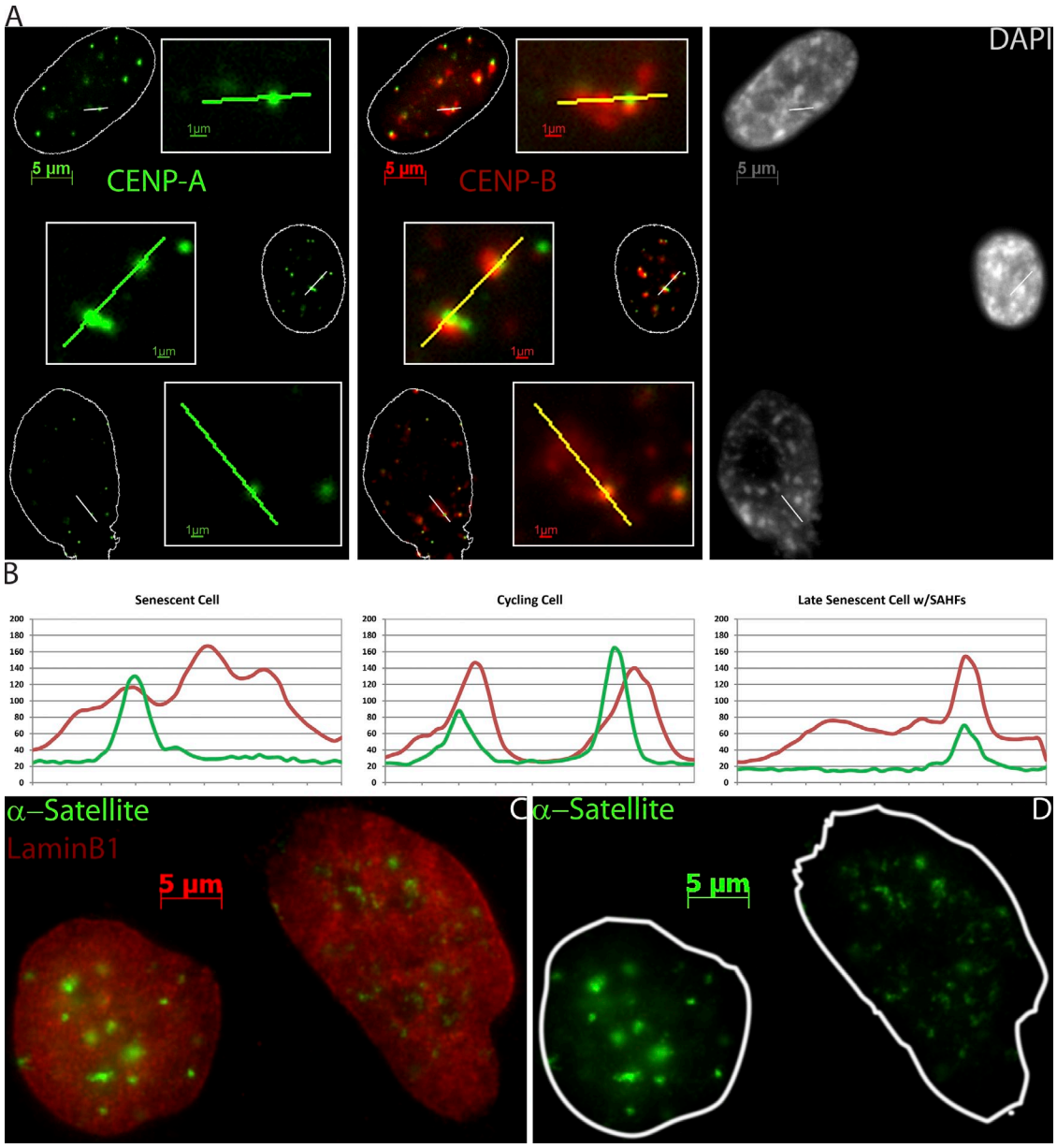

Figure S2. **CENP-A and -B distribution on individual centromeres of senescent cells and LaminB1 levels in cycling and senescent cells.** (A) CENP-A and -B staining in a senescent cell (top), cycling cell (middle), and late senescent cell with prominent SAHF (bottom). CENP-B staining distends in senescent cells (red), whereas CENP-A (green) does not. CENP-A staining levels on individual centromeres showed some variability, but were generally brighter in cycling and early senescent cells (middle and top) than late senescent cells (bottom). This is quantified by a line scan (expanded regions in A) shown in B where signal intensities (CENP-A, green; CENP-B, red) are plotted along the length of the drawn line. (C and D) LaminB1 (red) levels are not always lower in cells with distended satellites (green).

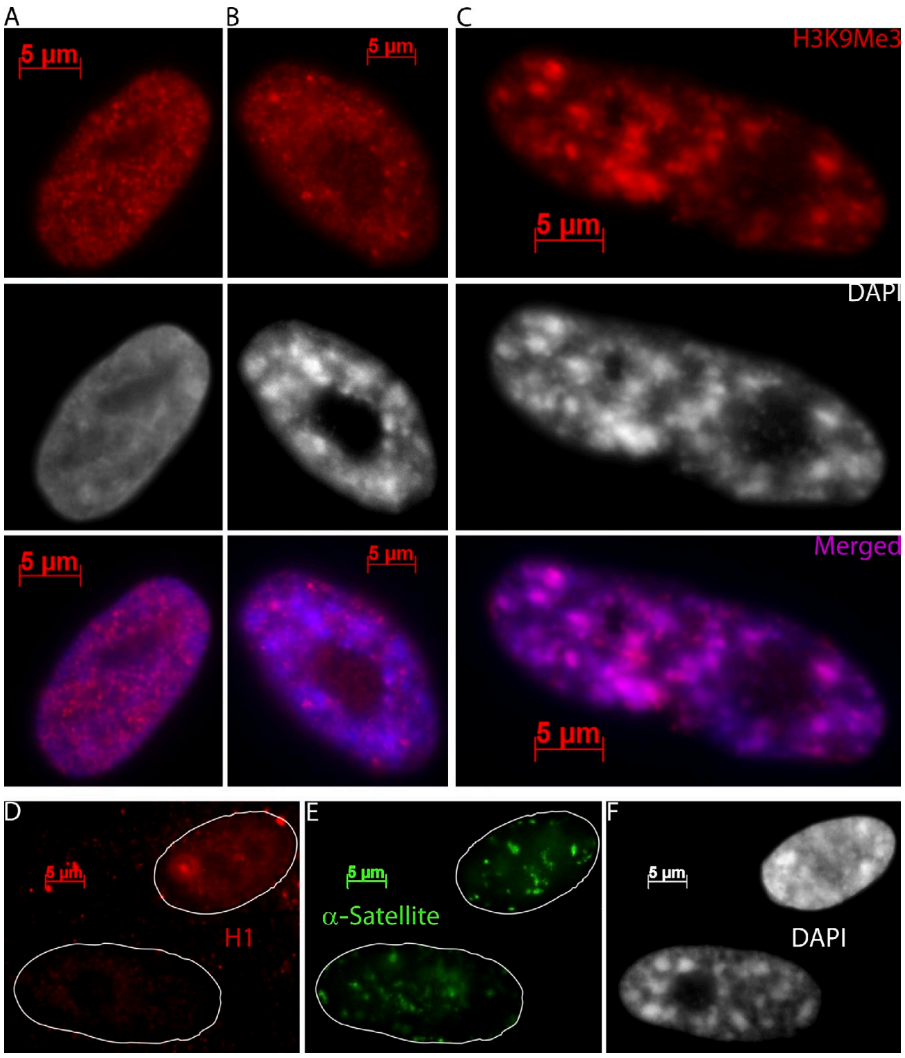

Figure S3. **H3K9Me3 distribution changes and H1 levels decrease with senescence.** H3K9Me3 (red) has a general nucleoplasmic signal in cycling (A, top) and senescent cells (B, middle). H3K9Me3 overlaps SAHF (DAPI) in late senescent cells (C, right). (D–F) Although both cells have distended α-sat (green), the top cell lacks SAHF (DAPI) and has robust H1 staining (red; 64%) and the bottom cell has SAHF and severely diminished H1 staining.

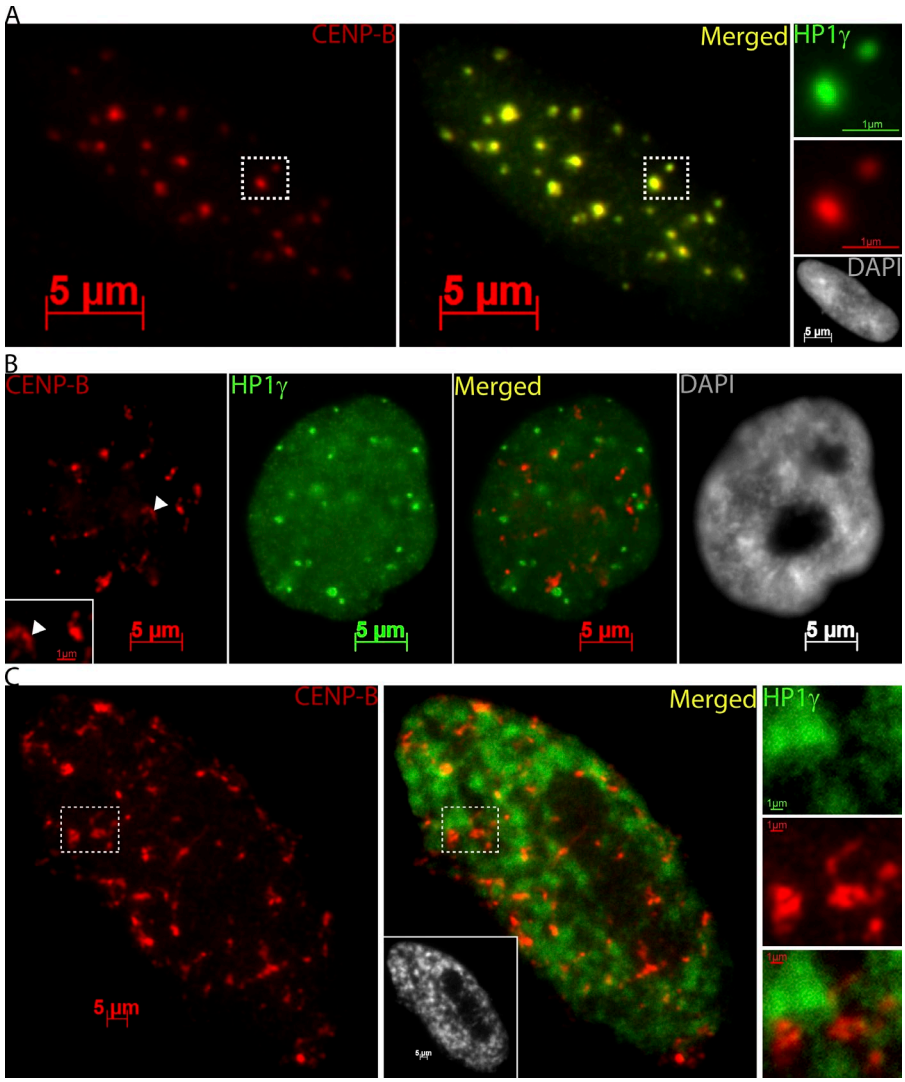

Figure S4. **HP1γ redistributes from satellites to SAHF as cells undergo senescence.** (A and B) HP1γ (green) and CENP-B (red) colocalize in cycling cells with condensed centromeres (A) but not in cells with distended centromeres (B) in which HP1γ gathers at PML bodies and no longer colocalizes with the centromeres. The arrowhead indicates a particularly decondensed centromere (magnified in the inset). The merged image in B combines two different planes. (C) In late stage senescent cells, HP1γ colocalizes with SAHF (DAPI; gray inset) and centromeres are often found in areas that lack intense HP1γ staining (magnified on right).

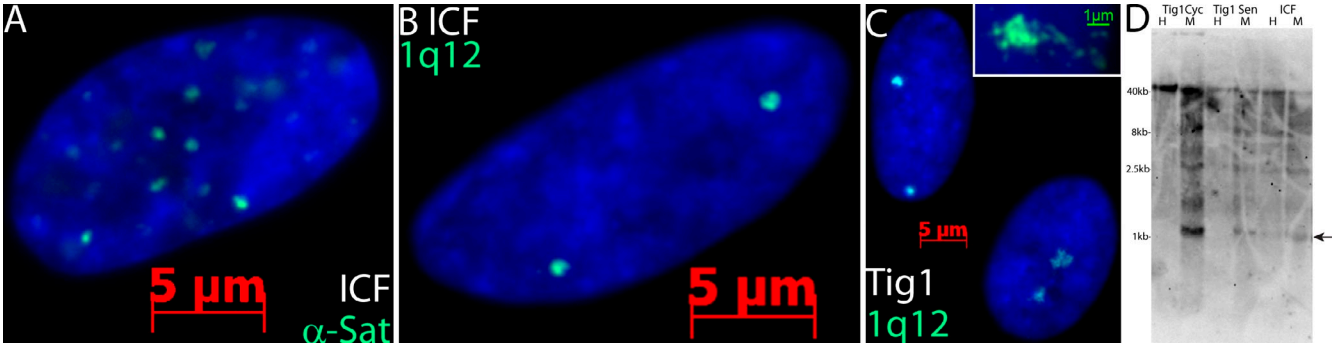

Figure S5. **Effects of hypomethylation on satellite distension.** (A and B) Cycling ICF cells do not display SADS or marked distension of nuclear α-sat (A) or sat II (B) on 1q12. (C) Appearance of sat II 1q12 (green) signals that distend in senescent Tig1 fibroblasts (bottom right), but are compact in cycling cells (top left). The inset shows a separate senescent cell with 1q12 signal that extends to the nuclear periphery. (D) A DNA methylation-sensitive Southern blot with ICF, senescent Tig1, and cycling Tig1 cells digested by HpaII (H) or MspI (M) and detected with a probe for sat II 1q12 sequences. The arrow points to a band size that is lacking in some of the methylation-sensitive HpaII lanes, indicating that the 1q12 region is methylated in the corresponding cell types. It is important to note that 1q12 remains methylated in both cycling and senescent cells.

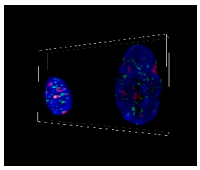

Video 1. **A 3D rendering of Fig. 1 A.** The video depicts a 3D reconstruction of Fig. 1 A created using Axiovision software where a cycling (left) and senescent (right) cell are hybridized with α-sat (green) and sat II (red) in DAPI-stained nuclei.

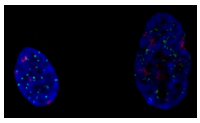

Video 2. **A Z stack from Fig. 1 A.** A cycling (left) and senescent (right) cell hybridized with α-sat (green) and sat II (red) in DAPI-stained nuclei. Each frame correlates to a successive slice (~0.1–0.25-µm apart) in the Z stack obtained with Axiovision software.